

# A Simple Model for the Oscillatory Iodate Oxidation of Sulfite and Ferrocyanide

Vilmos Gáspár<sup>†</sup> and Kenneth Showalter\*

Department of Chemistry, West Virginia University, Morgantown, West Virginia 26506-6045  
(Received: December 27, 1989; In Final Form: February 9, 1990)

A four-variable reduced model is developed from an empirical rate law model for the oscillatory iodate-sulfite-ferrocyanide reaction. The dynamical behavior of the reduced model is compared to that of the original 10-variable model and to the behavior found in experimental studies. The four-variable model is further reduced to a minimal two-variable model which retains most of the dynamical features of the original system. The transitions from oscillatory to steady-state behavior are examined in both reduced models, revealing an apparent infinite period bifurcation and a canard associated with a supercritical Hopf bifurcation.

## Introduction

The iodate oxidation of sulfite (the Landolt<sup>1</sup> clock reaction) and the related iodate oxidations of arsenous acid and ferrocyanide<sup>2</sup> are characterized by a long period of slow reaction followed by a rapid conversion of reactants to products. The iodate-ferrocyanide reaction is autocatalytic in iodide while the iodate-sulfite and iodate-arsenous acid reactions are autocatalytic in both iodide and hydrogen ion.

Interest in iodate clock reactions was renewed about 10 years ago with the discovery of "oligo-oscillatory" behavior in the iodate-sulfite-malonic acid reaction.<sup>3</sup> Three extrema in the concentration of iodide occur in this system prior to the final approach to equilibrium. Interest has also developed in recent years in the iodate-arsenous acid reaction as a model system for studies of bistability<sup>4,5</sup> and propagating reaction-diffusion fronts.<sup>6,7</sup>

Exactly 100 years after Landolt reported his clock reaction,<sup>1</sup> Edblom, Orbán, and Epstein<sup>8</sup> (EOE) reported that the iodate oxidation of sulfite in a CSTR becomes oscillatory when ferrocyanide is added to the reactant stream. A mechanism consisting of component oxidation-reduction reactions was proposed by EOE to explain the oscillatory behavior.

In ref 9, we reported on experiments further characterizing the iodate-sulfite-ferrocyanide system and the development of a dynamical model based on the component process description of EOE.<sup>8</sup> Rate laws and associated rate constants taken from literature accounts of each of the component processes were combined according to the stoichiometry of each process. The resulting empirical rate law model was nonoscillatory; however, when embellished with a buffer system comprised of the oxysulfur species of the reaction, it exhibits oscillations in pH strikingly similar to the measured behavior. The qualitative features of the transitions between oscillatory and steady-state behavior are also well described. In addition, the empirical rate law (ERL) model provides the basis for a detailed mechanism in terms of elementary steps.<sup>9</sup> An independent study by Edblom et al.<sup>10</sup> resulted in a mechanism similar to our own in most major aspects.

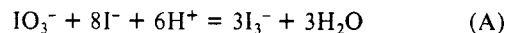
In order to develop a better understanding of the dynamical behavior of a complex system like the oscillatory iodate-sulfite-ferrocyanide (EOE<sup>11</sup>) reaction, it is useful to construct a reduced model with a minimum number of dynamic variables. The variables of the reduced model identify the chemical species of primary importance to the dynamical behavior, and the characterization of bifurcation points and other dynamical features is greatly facilitated by a model with few variables. Simple models of oscillatory reactions based on actual chemistry are rare, and a comparison of the dynamical features of such models is an effective approach for developing a general understanding of oscillatory behavior. In this paper, we present a reduction of our original ten-variable ERL model to a four-variable model that does a remarkably good job of describing the dynamical behavior of the oscillatory EOE reaction. We then show that the basic

features of the system can be accounted for by just two dynamic variables.

## Empirical Rate Law Model

Our ERL model<sup>9</sup> of the oscillatory EOE reaction was based on the following five component processes, most of which were originally identified by Edblom, Orbán, and Epstein.<sup>8</sup>

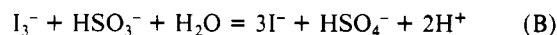
Process A is the iodate oxidation of iodide, first studied by Dushman<sup>12</sup> over 80 years ago. Rate law  $\alpha$  was developed by Liebafsky and Roe<sup>13</sup> in a review of the many studies of the Dushman reaction over the years.



$$R_\alpha = (k_{\alpha 1}[\text{I}^-] + k_{\alpha 2}[\text{I}^-]^2)[\text{IO}_3^-][\text{H}^+]^2 \quad (\alpha)$$

Process A as well as processes B and C are written in terms of triiodide ion since the concentration of iodide is always greater than that of iodine during the course of an oscillation. However, because iodine and triiodide in the presence of excess iodide are in rapid equilibrium, the component processes could be expressed in terms of either species.

Process B is the iodine oxidation of bisulfite, studied by Büнау and Eigen<sup>14</sup> using flow methods. They found a two-term rate law corresponding to the oxidation of bisulfite by iodine and the triiodide ion.



$$R_\beta = (k_{\beta 1}[\text{I}_3^-] + k_{\beta 2}[\text{I}_3^-]/K[\text{I}^-])[\text{HSO}_3^-] \quad (\beta)$$

Process C is the iodine oxidation of ferrocyanide, studied by Reynolds<sup>15</sup> in the late 1950s. He found no evidence of ferrocyanide oxidation by  $\text{I}_3^-$  and, in a limited range of acidity, no dependence on hydrogen ion. Rate law  $\gamma$  describes the forward and reverse

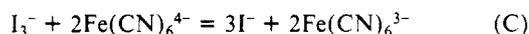
- 
- (1) Landolt, H. *Ber. Dtsch. Chem. Ges.* **1886**, *19*, 1317.
  - (2) Eggert, J.; Scharnow, B. *Z. Electrochem.* **1921**, *27*, 455.
  - (3) Rábai, Gy.; Bazsa, Gy.; Beck, M. T. *J. Am. Chem. Soc.* **1979**, *101*, 6746.
  - (4) Laplante, J. P. *J. Phys. Chem.* **1989**, *93*, 3882.
  - (5) Ganapathisubramanian, N.; Reckley, J. S.; Showalter, K. *J. Chem. Phys.* **1989**, *91*, 938.
  - (6) Hanna, A.; Saul, A.; Showalter, K. *J. Am. Chem. Soc.* **1982**, *104*, 3838.
  - (7) Sevcikova, H.; Marek, M. *J. Phys. Chem.* **1984**, *88*, 2181.
  - (8) Edblom, E. C.; Orbán, M.; Epstein, I. R. *J. Am. Chem. Soc.* **1986**, *108*, 2826.
  - (9) Gáspár, V.; Showalter, K. *J. Am. Chem. Soc.* **1987**, *109*, 4869.
  - (10) Edblom, E. C.; Györgyi, L.; Orbán, M.; Epstein, I. R. *J. Am. Chem. Soc.* **1987**, *109*, 4876.
  - (11) We refer to the oscillatory iodate-sulfite-ferrocyanide reaction as the EOE reaction in honor of its discoverers Edblom, Orbán, and Epstein.<sup>8</sup>
  - (12) Dushman, S. *J. Phys. Chem.* **1904**, *8*, 453.
  - (13) Liebafsky, H. A.; Roe, G. M. *Int. J. Chem. Kinet.* **1979**, *11*, 693.
  - (14) Büнау, G. V.; Eigen, M. *Z. Phys. Chem.* **1962**, *32*, 27.
  - (15) Reynolds, W. L. *J. Am. Chem. Soc.* **1958**, *80*, 1830.

<sup>†</sup> Permanent address: Department of Physical Chemistry, Kossuth L. University, P.O. Box 7, 4010 Debrecen, Hungary.

TABLE I: Four-Variable Model

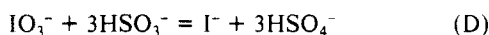
Process A	
$\{IO_3^-\} + \{I^-\} + 6H^+ \xrightarrow{k_{a2}} 3I_2 + \{3H_2O\}$	$6Y \xrightarrow{k_{a'}} 3Z$ (A')
$v_\alpha = -1/6 d[H^+]/dt = 1/3 d[I_2]/dt$	$v_{\alpha'} = -1/6 dY/dt = 1/3 dZ/dt$
$v_\alpha = \{k_{a2}(C_{IO_3^-})(C_{I^-})^2\}[H^+]^2$	$v_{\alpha'} = k_{\alpha'}Y^2$
	$2Y \xrightarrow{k_{N3}} Z$ (N3)
	$v_{N3} = -1/2 dY/dt = dZ/dt$
	$v_{N3} = 3k_{\alpha'}Y^2 = k_{N3}Y^2$
Process B	
$I_2 + HSO_3^- + \{H_2O\} \xrightarrow{k_\beta} \{2I^-\} + \{SO_4^{2-}\} + 3H^+$	$Z + X \xrightarrow{k_{N4}} 3Y$ (N4)
$v_\beta = k_\beta[I_2][HSO_3^-]$	$v_{N4} = k_{N4}ZX$
Process C	
$I_2 + \{2Fe(CN)_6^{4-}\} \xrightarrow{k_\gamma} \{2I^-\} + \{2Fe(CN)_6^{3-}\}$	$Z \xrightarrow{k_{N5}}$ (N5)
$v_\gamma = k_\gamma[I_2]C_{Fe(CN)_6^{4-}}$	$v_{N5} = k_{N5}Z$
Process D	
$\{IO_3^-\} + 3HSO_3^- \xrightarrow{k_\delta} \{I^-\} + \{3SO_4^{2-}\} + 3H^+$	$3X \xrightarrow{k_{\delta'}} 3Y$ (D')
$v_\delta = -1/3 d[HSO_3^-]/dt = 1/3 d[H^+]/dt$	$v_{\delta'} = -1/3 dX/dt = 1/3 dY/dt$
$v_\delta = k_\delta C_{IO_3^-}[HSO_3^-]$	$v_{\delta'} = k_{\delta'}X$
	$X \xrightarrow{k_{N2}} Y$ (N2)
	$v_{N2} = -dX/dt = dY/dt$
	$v_{N2} = 3k_{\delta'}X = k_{N2}X$
Process E2	
$SO_3^{2-} + H^+ \xrightleftharpoons[k_{-e2}]{k_{e2}} HSO_3^-$	$A + Y \xrightleftharpoons[k_{-N1}]{k_{N1}} X$ (N1)
$v_{e2} = k_{e2}[SO_3^{2-}][H^+]$	$v_{N1} = k_{N1}AY$
$v_{-e2} = k_{-e2}[HSO_3^-]$	$v_{-N1} = k_{-N1}X$

reactions for concentrations typical of the oscillatory EOE reaction.<sup>9</sup>



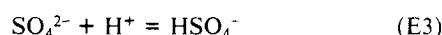
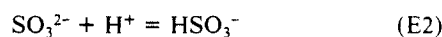
$$R_\gamma = \frac{k_\gamma[I_3^-][Fe(CN)_6^{4-}]^2}{K[I^-][Fe(CN)_6^{4-}]_0 - \frac{k_{-\gamma}([Fe(CN)_6^{4-}]_0 - [Fe(CN)_6^{4-}])^2[I^-]^2}{[Fe(CN)_6^{4-}]_0}} \quad (\gamma)$$

Process D is the uncatalyzed direct reaction between iodate and bisulfite. We assume a second-order rate law and evaluate the rate constant from measurements of the "Landolt time" by EOE.<sup>8,9</sup>



$$R_\delta = k_\delta[IO_3^-][HSO_3^-] \quad (\delta)$$

The weak acid equilibria of the oxysulfur species of the system are given by reactions E. This buffer system is continually titrated



$$R_{e1} = k_{e1}[HSO_3^-][H^+] - k_{-e1}[H_2SO_3] \quad (\epsilon 1)$$

$$R_{e2} = k_{e2}[SO_3^{2-}][H^+] - k_{-e2}[HSO_3^-] \quad (\epsilon 2)$$

$$R_{e3} = k_{e3}[SO_4^{2-}][H^+] - k_{-e3}[HSO_4^-] \quad (\epsilon 3)$$

by the oxidation-reduction processes A, B, and C and it in turn affects the rates of these processes. The buffer system is an

essential ingredient of the ERL model. Rate constants for the reactions are either known or can be readily estimated.<sup>9,16</sup>

The empirical rate law model is constructed by writing a differential equation for each of the variable species in the rate laws.<sup>9</sup> The production and consumption of each species is defined in terms of the stoichiometry and rate law of each process. Eleven species result in a 10-variable dynamical model, where the conservation of iron atoms allows elimination of one variable. The model could be further reduced to eight independent variables by considering conservation relations between species containing sulfur atoms and between species containing iodine atoms.

### Reduced Model

Our reduction of the 10-variable ERL model is based on the features of this model determined in our earlier study. Each of the component processes is simplified according to the prescription given in Table I. The simplifications are based on the following considerations:

1. In order to simplify the stoichiometry of the reduced model, each process is expressed in terms of iodine with the triiodide equilibrium incorporated appropriately into the rate laws.

2. Of the weak acid equilibria involving the oxysulfur species, only the equilibrium between  $HSO_3^-$  and  $SO_3^{2-}$  is retained. Equilibria E1 and E3 are neglected because they are relatively unimportant over the pH range of a typical oscillation.

3. The concentrations of iodate, iodide, ferrocyanide, and sulfate are in large excess and vary little over the course of an oscillation.

(16) Smith, R. M.; Martell, A. E. *Critical Stability Constants*; Plenum Press: New York, 1976; Vol. 4.

The concentrations of these species are therefore treated as constants and incorporated into the rate constants.

These simplifications result in a four-variable model given by reactions N1–N5. The variables of the reduced model and the corresponding species of the chemical reaction are identified by  $A \equiv \text{SO}_3^{2-}$ ,  $X \equiv \text{HSO}_3^-$ ,  $Y \equiv \text{H}^+$ , and  $Z \equiv \text{I}_2$ .



Table I shows the component processes in the left-hand column and the corresponding reduced descriptions in the right-hand column. The stoichiometries of the reduced descriptions reflect the variable species in the component processes. The species in braces are considered to be at constant concentrations and are indicated by  $C_i$  in the rate laws. The symbols for the reduced model are also used to indicate concentrations in the corresponding reduced rate laws.

Reaction N1 corresponds to the sulfite–bisulfite weak acid equilibrium, process E2. Reaction N2 corresponds to the direct, uncatalyzed iodate oxidation of bisulfite, process D. Because the concentrations of  $\text{IO}_3^-$ ,  $\text{I}^-$ , and  $\text{SO}_4^{2-}$  are essentially constant, process D effectively becomes the conversion of  $\text{HSO}_3^-$  to  $\text{H}^+$ , with the rate pseudo first order in bisulfite. The resulting reaction given by eq D' in Table I is further simplified by dividing by a factor of 3 to yield reaction N2. The stoichiometric factor is appropriately absorbed into the rate constant  $k_{\text{N2}}$ , and the rate expression  $v_{\text{N2}}$  now reflects the rate expression  $v_D$  for process D. Reaction N3 corresponds to process A, the Dushman reaction. For typical iodide concentrations of the EOE reaction, the first term in rate law  $\alpha$  is negligible, and only the second term is retained. Because the concentrations of  $\text{IO}_3^-$  and  $\text{I}^-$  are effectively constant, the process reduces to the conversion of hydrogen ion to molecular iodine at a rate pseudo second order in  $\text{H}^+$ . The stoichiometry of the corresponding eq A' is simplified by dividing by a factor of 3 to give reaction N3. This factor is absorbed into the rate constant  $k_{\text{N3}}$ , and again we note that the rate expression  $v_{\text{N3}}$  reflects the kinetics of process A. Reaction N4 corresponds to process B, the iodine oxidation of bisulfite. This process reduces to the reaction of iodine with bisulfite to generate hydrogen ion, since the concentrations of  $\text{I}^-$  and  $\text{SO}_4^{2-}$  are effectively constant. For the iodide concentrations typical in the oscillatory reaction, the first term in rate law  $\beta$  is dominant and is used to calculate the apparent rate constant. The resulting rate law is first order in bisulfite and first order in iodine. Reaction N5 corresponds to process C, the iodine oxidation of ferrocyanide. This process reduces to a first-order decay of iodine, since the concentrations of ferrocyanide and iodide are effectively constant and ferricyanide is kinetically unimportant.

The ordinary differential equations corresponding to the system in a CSTR are given by eqs 1–4.

$$dX/dt = k_{\text{N1}}AY - k_{\text{N1}}X - k_{\text{N2}}X - k_{\text{N4}}ZX - k_0X \quad (1)$$

$$dY/dt = -k_{\text{N1}}AY + k_{\text{N1}}X + k_{\text{N2}}X - 2k_{\text{N3}}Y^2 + 3k_{\text{N4}}ZX + k_0(Y_0 - Y) \quad (2)$$

$$dZ/dt = k_{\text{N3}}Y^2 - k_{\text{N4}}ZX - k_{\text{N5}}Z - k_0Z \quad (3)$$

$$dA/dt = -k_{\text{N1}}AY + k_{\text{N1}}X + k_0(A_0 - A) \quad (4)$$

The reciprocal residence time of the reactor (flow rate/volume) is given by  $k_0$ . The input stream contains hydrogen ion and sulfite, which appear in eqs 2 and 4 as  $Y_0$  and  $A_0$ , respectively.

### Dynamical Behavior

The four-variable reduced model does a remarkably good job of reproducing the experimentally observed behavior.<sup>8,9</sup> Shown in Figure 1a is a plot of pH as a function of time; a blowup of

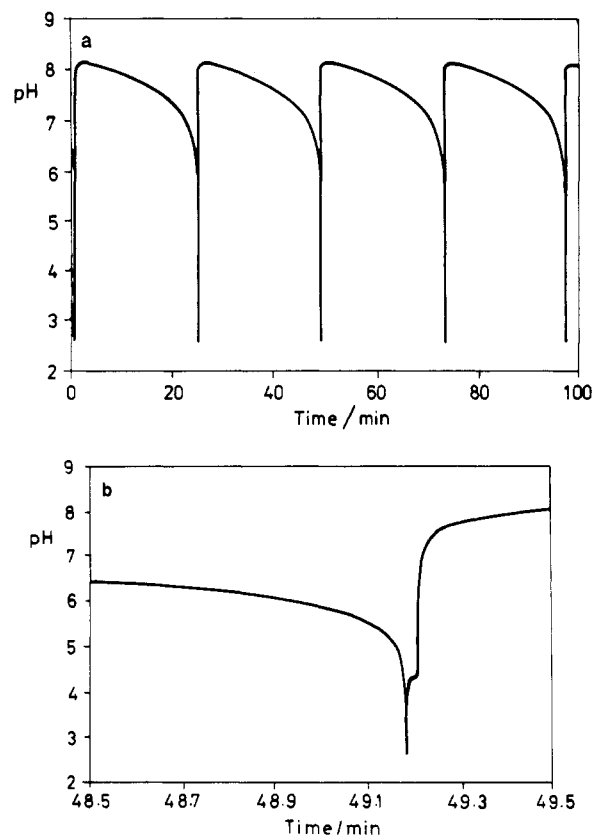


**Figure 1.** (a) pH as a function of time calculated from eqs 1–4 describing the four-variable model N1–N5. (b) Blowup of pH oscillation between 48.5 and 49.5 min. Values of rate constants and concentrations in Table II;  $Y_0 = 3.0 \times 10^{-3}$  M and  $k_0 = 1.5 \times 10^{-3}$  s<sup>-1</sup>.

**TABLE II: Values of Rate Constants and Concentrations**

Concentrations	
$[\text{IO}_3^-]_0$	$= 7.5 \times 10^{-2}$ M
$[\text{SO}_3^{2-}]_0$	$= 9.0 \times 10^{-2}$ M
$[\text{Fe}(\text{CN})_6^{4-}]_0$	$= 2.5 \times 10^{-2}$ M
$[\text{I}^-]_{\text{av}}$	$= 2.0 \times 10^{-2}$ M
$[\text{H}^+]_0$	$= 2[\text{H}_2\text{SO}_4]_0$ (varied)
Rate Constants	
$k_{\text{N1}} = k_{\text{t2}}$	$= 5.0 \times 10^{10}$ M <sup>-1</sup> s <sup>-1</sup>
$k_{-\text{N1}} = k_{-\text{t2}}$	$= 8.1 \times 10^3$ s <sup>-1</sup>
$k_{\text{N2}} = 3k_D[\text{IO}_3^-]_0$	$= 6.0 \times 10^{-2}$ s <sup>-1</sup>
$k_{\text{N3}} = k_{\alpha 2}[\text{IO}_3^-]_0[\text{I}^-]_{\text{av}}^2$	$= 7.5 \times 10^4$ M <sup>-1</sup> s <sup>-1</sup>
$k_{\text{N4}} = k_{\beta 2}$	$= 2.3 \times 10^9$ M <sup>-1</sup> s <sup>-1</sup>
$k_{\text{N5}} = k_{\gamma}[\text{Fe}(\text{CN})_6^{4-}]_0$	$= 3.0 \times 10^1$ s <sup>-1</sup>
$k_0$	= reciprocal residence time (varied)

the behavior near the pH minimum is shown in Figure 1b. The broad maximum and sharp minimum of the pH oscillation as well as the plateau at  $\text{pH} \approx 4.25$  are in very good agreement with experiment; agreement with the 10-variable ERL model is also good.<sup>9</sup> (Values of the rate constants and other parameters used in the calculations are listed in Table II; see ref 9 for sources of the rate constants.)

Figure 2 shows the amplitude and period of the pH oscillations calculated as a function of the feedstream hydrogen ion concentration. Also shown is the pH of the flow (low  $[\text{H}^+]_0$ ) and thermodynamic (high  $[\text{H}^+]_0$ ) branches of steady states. Again, agreement with experiment is very good,<sup>9</sup> although a quantitative discrepancy in the range of oscillatory behavior is apparent. (Modifications of the model designed to remove such discrepancies are discussed below.) The dramatic increase in period on decreasing  $[\text{H}^+]_0$  mirrors the experimentally observed behavior. Such a divergence in period as oscillations give way to steady-state behavior is diagnostic of an infinite-period bifurcation.<sup>17</sup> On

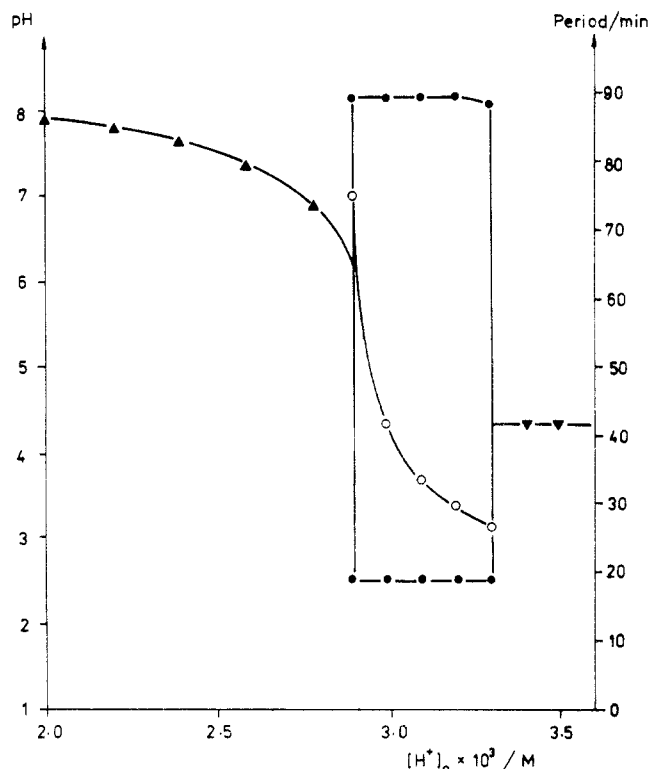


**Figure 2.** Calculated amplitude (●) and period (○) of pH oscillations as a function of  $[H^+]_0$ . Steady-state pH of flow branch (▲) and thermodynamic branch (▼) shown bracketing oscillatory region. Values of rate constants and concentrations in Table II;  $k_0 = 2.0 \times 10^{-3} \text{ s}^{-1}$ .

**TABLE III: Minimum and Maximum pH, Amplitude, and Period of Oscillation as a Function of  $Y_0^a$**

$10^3 Y_0 / \text{M}$	$\text{pH}_{\min}$	$\text{pH}_{\max}$	$\Delta \text{pH}$ (amplitude)	period
3.30	2.5	8.07	5.57	26.25 min
3.31	2.5	8.07	5.57	26.25 min
3.32	2.5	8.07	5.57	26.25 min
3.321	4.2977	4.3107	0.0130	0.910 s
3.325	4.2981	4.3106	0.0125	0.900 s
3.33	4.2986	4.3104	0.0118	0.894 s
3.34	4.2995	4.3100	0.0105	0.879 s
3.35	4.3004	4.3096	0.0092	0.865 s
3.36	4.3013	4.3092	0.0079	0.851 s
3.37	4.3023	4.3087	0.0064	0.839 s
3.38	4.3034	4.3080	0.0046	0.829 s
3.39	4.3049	4.3068	0.0019	0.818 s
3.3924	4.3059 <sup>b</sup>			

<sup>a</sup>Oscillations undergo large changes in amplitude and period at canard ( $Y_0 \approx 3.32 \times 10^{-3} \text{ M}$ ) and terminate at supercritical Hopf bifurcation ( $Y_0 = 3.3924 \times 10^{-3} \text{ M}$ ). <sup>b</sup>Steady-state pH.

increasing  $[H^+]_0$ , the abrupt transition from large-amplitude oscillations to the thermodynamic branch of steady states is suggestive of a subcritical Hopf bifurcation. However, higher resolution calculations show that the transition is more complicated. The large-amplitude, low-frequency oscillations are suddenly transformed to small-amplitude, high-frequency oscillations, which eventually terminate on increasing  $[H^+]_0$  in a supercritical Hopf bifurcation. The amplitude and period of the pH oscillations as the system undergoes this apparent canard are given in Table III. A *canard* is a *false* bifurcation because, even though the quantitative behavior undergoes a dramatic change, the qualitative dynamical features remain unchanged.<sup>18,19</sup> Thus, while the period and amplitude of oscillation undergo a major transformation at the canard, the system remains oscillatory. A similar canard was

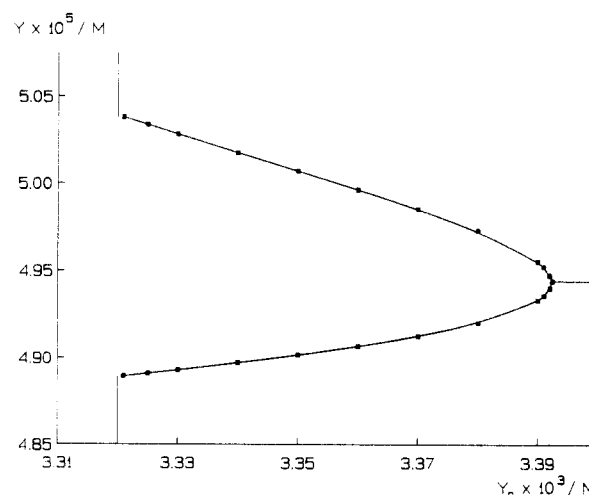


**Figure 3.** Blowup of transition from oscillatory to steady-state behavior at high  $Y_0$  shown in Figure 2. Amplitude of oscillations in  $Y$  and steady-state concentration shown as a function of input concentration  $Y_0$ . Vertical lines at  $Y_0 \approx 3.32 \times 10^{-3} \text{ M}$  represent canard.

found in the 10-variable ERL model.<sup>9</sup>

Shown in Figure 3 is a blowup of the maximum and minimum in  $Y$  at values of  $Y_0$  beyond the canard. The nearly vertical lines at  $Y_0 \approx 3.32 \times 10^{-3} \text{ M}$  represent the canard, where both the amplitude and period decrease by more than 3 orders of magnitude. The smoothly diminishing amplitude and nearly constant period on increasing  $Y_0$  beyond the canard (listed in Table III) are diagnostic of a supercritical Hopf bifurcation. Plots of  $\log(Y_{\max} - Y_{\min})$  vs  $\log Y_0^*$ , where  $Y_0^*$  is the displacement from the bifurcation point, are reasonably linear with slopes approaching  $-1/2$  as  $Y_0^*$  approaches zero; a least-squares slope of  $-0.54$  was calculated using the last six values of  $Y_0$  in Figure 3 before the bifurcation point. An amplitude dependence on  $(Y_0^*)^{-1/2}$  and a nearly constant period show that the oscillatory behavior is terminated at a typical supercritical Hopf bifurcation.

### Three-Variable Reduction

Three dynamic variables are necessary for a model with only uni- and bimolecular steps to exhibit limit cycle oscillations.<sup>20,21</sup> It is of interest to determine whether the four-variable model can be further reduced and still retain the dynamical features necessary for oscillatory behavior. The reduction is facilitated by rewriting eqs 1–4 in terms of the dimensionless variables  $a$ ,  $x$ ,  $y$ , and  $z$  and dimensionless time  $\tau$ .

$$dx/d\tau = ay - x - xz - \xi x \quad (5)$$

$$dy/d\tau = -ay + x - y^2 + 3xz - \xi y + \eta Y_0 \quad (6)$$

$$dz/d\tau = \psi y^2 - 2\psi xz - \kappa z - \xi z \quad (7)$$

$$da/d\tau = -\lambda ay + \lambda \mu x - \xi a + \lambda \eta A_0 \quad (8)$$

In eqs 5–8,  $A_0$  and  $Y_0$  are input concentrations as earlier defined and the parameters, with  $k_0 = 1.5 \times 10^{-3} \text{ s}^{-1}$ , are given by

$$\xi = k_0 / (k_{-N1} + k_{N2}) = 1.9 \times 10^{-7}$$

$$\eta = 2k_0 k_{N3} / (k_{-N1} + k_{N2})^2 = 3.4 \times 10^{-6} \text{ M}^{-1}$$

$$\psi = k_{N4} / 4k_{N3} = 7.7 \times 10^3$$

$$\kappa = k_{N5} / (k_{-N1} + k_{N2}) = 3.7 \times 10^{-3}$$

$$\lambda = k_{N1} / 2k_{N3} = 3.3 \times 10^5$$

$$\mu = k_{-N1} / (k_{-N1} + k_{N2}) = 1.0$$

An examination of the values of the parameters in eqs 5–8 reveals

(18) Thompson, J. M. T.; Stewart, H. B. *Nonlinear Dynamics and Chaos*; Wiley: New York, 1986.

(19) Diener, M. *Math. Intell.* **1984**, *6*, 38.

(20) Tyson, J. J.; Light, J. C. *J. Chem. Phys.* **1973**, *59*, 4164.

(21) Hanusse, P. *C. R. Acad. Sci., Ser. C* **1972**, *274*, 1245.

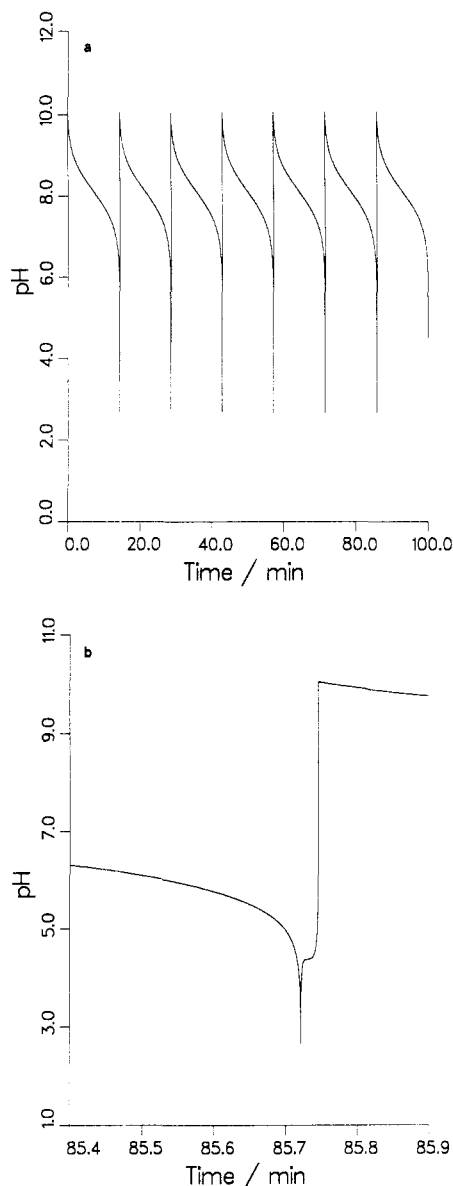


**Figure 4.** (a) pH as a function of time calculated from the two-variable reduction of model N1–N5. (b) Blowup of pH oscillation between 85.4 and 85.9 min. Values of rate constants and concentrations in Table II;  $Y_0 = 3.0 \times 10^{-3}$  M and  $k_0 = 1.5 \times 10^{-3}$  s $^{-1}$ .

that  $a$  is a fast variable in the model. Because  $a$  relaxes more rapidly than the much slower variables  $x$  and  $y$ , it can be approximated as an instantaneous function of these variables. Setting  $da/d\tau = 0$  in eq 8 gives  $a$  as a function of  $x$  and  $y$ , according to

$$a(x,y) = \frac{\lambda\eta A_0 + \lambda\mu x}{\xi + \lambda y} \quad (9)$$

The resulting three-variable model is oscillatory with behavior similar in most aspects to its parent four-variable model. Because this model exhibits behavior similar to that of a two-variable reduction discussed below, it is regarded as an intermediate result and is not considered further.

#### Two-Variable Reduction

Examining the relative magnitudes of the parameters in eqs 5–8 reveals that the variable  $z$  relaxes on a time scale comparable to that of the fast variable  $a$ . Setting  $dz/d\tau = 0$  in eq 7 gives  $z$  as a function of  $x$  and  $y$  according to

$$z(x,y) = \frac{\psi y^2}{2\psi x + \kappa + \xi} \quad (10)$$

An additional motivation for considering  $z$  as a function of  $x$  and

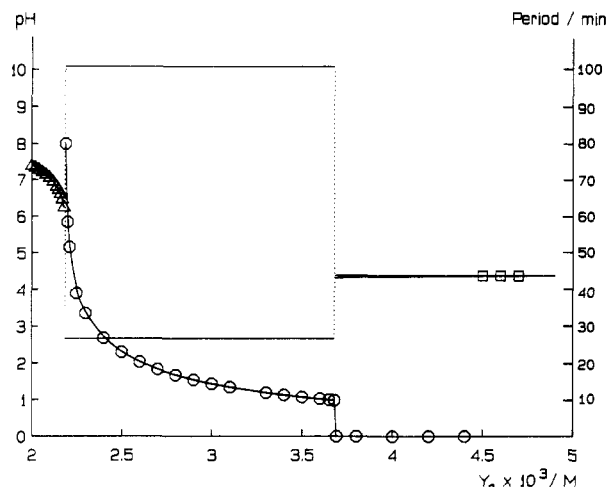


**Figure 5.** Amplitude (—) and period (O) of pH oscillations as a function of  $Y_0$  calculated from two-variable model. Steady-state pH of flow branch ( $\Delta$ ) and thermodynamic branch ( $\square$ ) shown bracketing oscillatory region. Values of rate constants and concentrations in Table II;  $k_0 = 1.5 \times 10^{-3}$  s $^{-1}$ .

$y$  is that, with this approximation, reactions N3 and N4 are effectively combined into a single step. The result is a reaction analogous to the cubic autocatalysis of the Autocatalator<sup>22</sup> and the related CSTR model<sup>23</sup> of Gray and Scott.

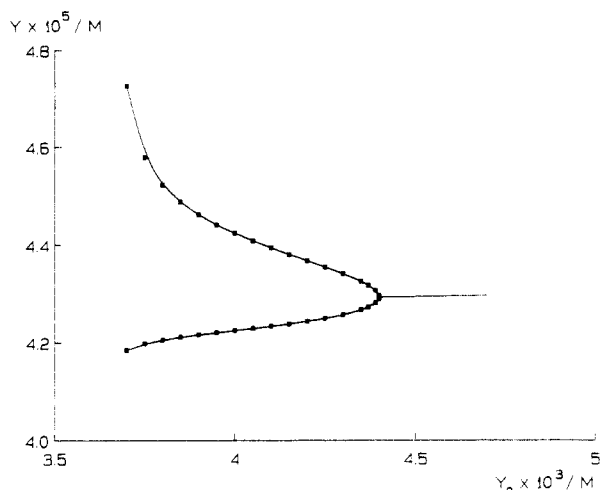
The resulting two-variable model of the EOE reaction quite remarkably reproduces almost all of the behavior of the original 10-variable model. Shown in parts a and b of Figure 4 are the oscillations in pH and a blowup of the behavior near the pH minimum of an oscillation. (Calculations were carried out with dimensioned variables in order to facilitate comparisons with the other model calculations.) The period is somewhat shorter than that generated by the four-variable model in Figure 1a; however, as discussed below, the qualitative trend in the period is in good agreement with the more complex models and experimental measurements. The features of the pH minimum are also very well reproduced by the two-variable model, as shown in Figure 4b. The rounded drop to a very sharp minimum followed by an interruption of the pH rise at a plateau are in nearly quantitative agreement with the four-variable behavior shown in Figure 1b. The sharp minimum and subsequent plateau were observed in all of our experimental measurements of pH as a function of time as well as in our 10-variable calculations.<sup>9</sup> The shape of the pH maximum is the only qualitative feature that the two-variable model fails to reproduce. The maximum is sharp rather than rounded as in Figure 1a as well as in the experimental measurements.

Figure 5 shows the period and amplitude of  $Y$  as a function of  $Y_0$  for the same reactant concentrations and a slightly different value of  $k_0$  used to calculate Figure 2 with the four-variable model. The qualitative features of the two figures are in very good agreement, and there is even semiquantitative agreement between some of the features. On decreasing  $Y_0$ , the period steadily increases to an apparent divergence at the transition to the flow-branch steady state. This apparent infinite-period bifurcation is amenable to detailed characterization with a two-variable model,<sup>17</sup> as we pursue elsewhere, and can be immediately identified as a saddle-loop bifurcation, as discussed below. On increasing  $Y_0$ , the canard seen in the more complex models is again exhibited.

Figure 6 shows a blowup of the amplitude in  $Y$  as  $Y_0$  is increased beyond the canard. We see that oscillations are terminated at a supercritical Hopf bifurcation in a manner similar to that found with the four-variable model. The Hopf bifurcation and the canard are much farther apart in the two-variable calculation than in the four-variable calculation. Figure 7 shows the period as a function of  $Y_0$  between the canard and the supercritical Hopf bifurcation.

(22) Gray, P.; Scott, S. K. *Ber. Bunsen-Ges. Phys. Chem.* **1986**, *90*, 985.

(23) Gray, P.; Scott, S. K. *J. Phys. Chem.* **1985**, *89*, 22.



**Figure 6.** Blowup of transition from oscillatory to steady-state behavior at high  $Y_0$  shown in Figure 5. Amplitude of oscillations in  $Y$  and steady-state concentration shown as a function of input concentration  $Y_0$ .

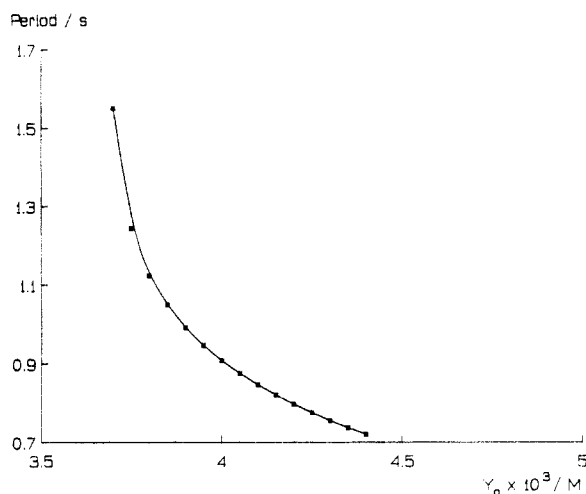


**Figure 7.** Period as a function of  $Y_0$  for small-amplitude oscillations in Figure 6.

We see the period increasing in a manner suggestive of an infinite-period bifurcation. Insights into this transition can be gained by examining the two-variable description using techniques that are difficult to implement with models containing more than two variables (e.g., backward integration). A characterization of the two-variable system in terms of the insets and outsets of the stationary states and how the oscillatory behavior is influenced by these states will reveal whether or not the canard is a pseudo-infinite-period bifurcation.

On decreasing  $Y_0$ , the period of oscillation increases and apparently diverges at the transition to the flow-branch stationary state. This behavior suggests that oscillations terminate at either a saddle-loop or saddle-node infinite-period bifurcation. The linear plot of period as a function of  $\log Y_0^*$  shown in Figure 8 indicates that oscillations are terminated at a saddle-loop bifurcation.<sup>24</sup>

### Discussion

The iodate-sulfite-ferrocyanide reaction was among the first oscillatory systems found to exhibit large-amplitude oscillations in the concentration of hydrogen ion.<sup>8</sup> As shown in Figure 1 and in experimental measurements that are very similar,<sup>8,9</sup> hydrogen ion concentration changes by more than 5 orders of magnitude during the course of an oscillation. It is also significant that the oscillations pass through  $\text{pH} = 7$ , resulting in a reaction mixture that changes between moderately acidic and mildly basic. A

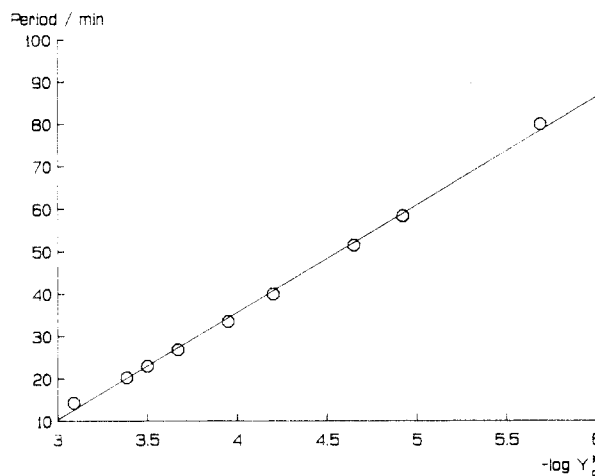


**Figure 8.** Period as a function of  $\log Y_0^*$  for large-amplitude oscillations in Figure 5.

number of CSTR systems are now known to exhibit large-amplitude oscillations in  $\text{H}^+$ .<sup>25-33</sup> The bromate-sulfite-ferrocyanide reaction<sup>32</sup> is the closest relative of the EOE reaction among these new oscillatory systems.

The EOE reaction is an exceptionally attractive system for detailed characterization. Few oscillatory systems are known with as many experimentally accessible chemical species.<sup>8</sup> Potentiometric measurements of  $\text{pH}$  and  $\text{I}^-$  are readily carried out,<sup>8,9</sup> and spectrophotometric measurements of  $\text{Fe}(\text{CN})_6^{4-}$ ,  $\text{Fe}(\text{CN})_6^{3-}$ ,  $\text{I}_2$ , and  $\text{I}_3^-$  are possible. The most important feature of the reaction is that it can be accurately described in terms of component reactions, as first proposed by EOE.<sup>8</sup> This component process description provided the foundation for our empirical rate law model<sup>9</sup> and also provided the basis for detailed descriptions in terms of elementary steps.<sup>9,10</sup>

The four-variable model N1-N5 has a number of features that are reminiscent of the Autocatalator<sup>22</sup> proposed by Gray and Scott as a prototype for oscillatory behavior in isothermal chemical systems. The two-variable Autocatalator is comprised of the following four reactions:



The decay of the precursor  $\text{P}$  to generate  $\text{A}$  is assumed to occur very slowly, allowing the concentration of  $\text{P}$  to be considered constant in a "pool chemical" approximation. The model A2-A4 without the initiation reaction A1 describes an oscillatory reaction in a CSTR,<sup>23</sup> where  $\text{A}$  and  $\text{B}$  are supplied by the reactant stream.

The similarities between reactions N1-N5 and A1-A4 become apparent when the two-variable reduction of the former is considered. The most important is reaction A3 of the Autocatalator and the combined steps N3 and N4, where the fast variable  $\text{Z}$  is treated as an instantaneous function of  $\text{X}$  and  $\text{Y}$  according to eq 10. The Autocatalator becomes a three-variable model when an intermediate is introduced in order to mimic the cubic autocatalysis by two bimolecular steps. A recent study of three-variable

(25) Beck, M. T.; Rábai, Gy. *J. Phys. Chem.* **1985**, *89*, 3907.

(26) Orbán, M.; Epstein, I. R. *J. Am. Chem. Soc.* **1985**, *107*, 2302.

(27) Rábai, Gy.; Nagy, Zs. V.; Beck, M. T. *React. Kinet. Catal. Lett.* **1987**, *33*, 23.

(28) Orbán, M.; Epstein, I. R. *J. Am. Chem. Soc.* **1987**, *109*, 101.

(29) Rábai, Gy.; Beck, M. T. *J. Phys. Chem.* **1988**, *92*, 2804.

(30) Rábai, Gy.; Kustin, K.; Epstein, I. R. *J. Am. Chem. Soc.* **1989**, *111*, 3870.

(31) Rábai, Gy.; Epstein, I. R. *J. Phys. Chem.* **1989**, *93*, 7556.

(32) Edblom, E. C.; Luo, Y.; Orbán, M.; Kustin, K.; Epstein, I. R. *J. Phys. Chem.*, in press.

(33) Rábai, Gy.; Beck, M. T.; Kustin, K.; Epstein, I. R. *J. Phys. Chem.* **1989**, *93*, 2853.

(24) Gaspard, P. *J. Phys. Chem.* **1990**, *94*, 1. Gaspard, P. Thesis, Université Libre de Bruxelles, 1987. Baensens, C. Thesis, Université Libre de Bruxelles, 1987.

Autocatalators demonstrated that step A3 can be replaced by several different sequences of bimolecular steps without altering the qualitative dynamical features of the model.<sup>34</sup> These bimolecular models, including one with an autocatalytic sequence identical with steps N3 and N4, demonstrate that the cubic step A3 embodies the essential elements of the autocatalysis.

Reactions N1–N5 and A1–A4 both have uncatalyzed pathways with the same stoichiometry as the autocatalytic pathways. Reaction N2 is the alternate pathway in the four-variable model, and reaction A2 is the alternate pathway in the Autocatalator. The decay of the autocatalyst in step A4 of the Autocatalator is replaced in model N1–N5 by the decay of the intermediate Z of the autocatalytic sequence N3 + N4 in step N5. The decay of the precursor P to generate A in step A1 of the Autocatalator is replaced in model N1–N5 by an equilibrium between A, Y, and X in step N1. We note, however, that this comparison is not appropriate since the Autocatalator is a batch reaction model while the four-variable model describes a CSTR system with both A and Y provided by the reactant stream. In the CSTR model eqs A2–A4, A and B are supplied by the reactant stream and no initiation step is necessary.<sup>23</sup> The equilibrium N1 is better compared with the initiation step of a reversible, three-variable CSTR model proposed by Li,<sup>35</sup> which is based on quadratic autocatalysis. In both models, the autocatalyst and the reactant consumed in autocatalysis, Y and X in model N1–N5, are in equilibrium.

A rational approach for improving model N1–N5 is to address deficiencies in the original 10-variable empirical rate law model. Several of the component processes of this model need to be reinvestigated to refine the rate constants and better establish the rate laws. Process C, the iodine oxidation of ferrocyanide, was studied by Reynolds<sup>15</sup> in neutral and mildly basic solutions; the rate law for this process needs to be reevaluated for solutions containing H<sup>+</sup> in concentrations comparable to those in the oscillatory reaction. Our original study showed that process C becomes important between the pH minimum (~3.5) and the plateau in the pH rise (~4.25).

Process D, the uncatalyzed direct reaction between iodate and bisulfite, also needs to be reevaluated. Rate law  $\delta$  follows from proposals that the reaction proceeds by successive oxygen atom transfers;<sup>1,2</sup> however, no direct evidence for this rate law is available. Studies of process D are complicated by the autocatalytic pathway A + 3B, which is usually the dominant pathway of the reaction. Our preliminary studies indicate that rate law  $\delta$  is a reasonably accurate description of the kinetics of process D.

Recent studies by Yiin and Margerum<sup>36</sup> indicate that the rate of process B, the bisulfite reduction of I<sub>2</sub> and I<sub>3</sub><sup>-</sup>, is actually much slower than that reported by Büнау and Eigen.<sup>14</sup> The earlier study apparently measured only the very rapid appearance of HSO<sub>3</sub>I, a reaction intermediate, and the much slower decay of this species

determines the rate of the overall reaction. Refinement of the rate constant for this process in light of the recent measurements may significantly improve the model.

Finally, Luo and Epstein<sup>37</sup> have proposed that the direct reaction between iodate and ferrocyanide plays an essential role in the oscillatory reaction as a negative feedback process. Because H<sup>+</sup> is consumed in this process, it might represent a decay of the autocatalyst Y in the reduced model, analogous to step A4 in the Autocatalator.

The basis of the original ERL model was a description of the oscillatory reaction in terms of the reasonably well established rate behavior of the component processes. Every rate law and rate constant making up the ERL model considered here was taken directly or indirectly from the literature, making the model unprecedented among models of oscillatory reactions in its lack of adjustable parameters. Extending this algorithm by refining the component process descriptions should lead to an improvement of the ERL model and an associated improvement of the reduced models.

### Conclusion

In this paper we have shown how an empirical rate law model of the oscillatory iodate–sulfite–ferrocyanide reaction can be reduced from 10 variables to 4 variables while retaining essentially all of the qualitative dynamical features. We have also shown that the four-variable description can be reduced to a description containing only two variables, the minimum number of variables necessary to describe oscillatory behavior. Remarkably, most of the qualitative features of the 10-variable model are found in the minimal model. In addition, interesting similarities between the minimal model and the Autocatalator can be identified. Finally, we have described how the ERL and reduced models can be improved by reexamining some of the component processes.

Perhaps the most attractive feature of the EOE reaction is that the oscillatory behavior is easy to understand in an intuitive sense, suggesting that this system might serve as a pedagogical example of chemical oscillators. The component processes are reactions that each have a long history in chemical kinetics, and together they form an oscillatory reaction that is mechanistically simple yet dynamically rich. The reaction can be described by a simple four-variable model, and it, in turn, can be described by just two dynamical variables.

*Acknowledgment.* This work was supported by the National Science Foundation (Grants CHE-8920664 and INT-8822786). We are grateful to the National Science Foundation and the Hungarian Academy of Sciences for support of a U.S.–Hungary Cooperative Science Project. We also thank Bo Peng for his assistance in developing the model in terms of dimensionless variables.

**Registry No.** IO<sub>3</sub><sup>-</sup>, 15454-31-6; SO<sub>3</sub><sup>2-</sup>, 14265-45-3; Fe(CN)<sub>6</sub><sup>4-</sup>, 13408-63-4.

(34) Aris, R.; Gray, P.; Scott, S. K. *Chem. Eng. Sci.* **1988**, *43*, 207.

(35) Li, R.-S. *J. Chem. Soc., Faraday Trans. 2* **1988**, *84*, 737.

(36) Yiin, B. S.; Margerum, D. W. *Inorg. Chem.* **1988**, *27*, 1670.

(37) Luo, Y.; Epstein, I. R. *J. Phys. Chem.* **1989**, *93*, 1398.